STRAINS AND FAILURE MODES IN HUMAN METASTATIC VERTEBRAE

Marco Palanca[1], Giulia Cavazzoni[1], Luca Cristofolini[1], Enrico Dall'Ara[2]
1. *Dept of Industrial Engineering, Alma Mater Studiorum – University of Bologna, Bologna, IT*
2. *Dept of Oncology and Metabolism and INSIGNEO, University of Sheffield, Sheffield, UK*

Introduction

Biomechanical studies [1, 2] have analysed the effects of bone metastases on the mechanical behaviour of the vertebrae, in order to improve our understanding of their risk of fracture. These studies provide remarkable insight about the overall mechanical properties of metastatic vertebrae, but how these lesions contribute to the failure process and failure pattern is still unclear. Micro-computed tomography (µCT) imaging and Digital Volume Correlation (DVC) provide unique quantitative assessments of the internal displacement and strain fields, and a clear identification of the failure mode and location of failure onset [3].

The aim of this study was to i) evaluate the local internal strain maps at failure in human metastatic and healthy vertebrae and ii) identify their different failure modes.

Methods

Fifteen four-vertebrae spine segments, consisting of a metastatic (6x lytic, 6x mixed or 3x blastic) and a healthy vertebra in the middle, were obtained from an ethically approved donation program. The most cranial and most caudal vertebrae were partially embedded in bone cement to hold the specimen in a hand-operated jig equipped with a load cell (HBK, 10kN). Each specimen was loaded in uniaxial compression, inside a µCT scanner (Scanco VivaCT80, isotropic voxel size = 39µm). Two scans of each specimen were acquired in zero-strain conditions to assess the DVC measurement uncertainty (standard deviation of the errors, SDER). Then, the specimens were loaded up to failure (first abrupt drop of the load) in order to measure the internal strains at failure. A global DVC approach (BoneDVC) [4], with a measurement spatial resolution of 1.95mm was used to measure the minimum principal strains (eps3). Percentage Strain Difference was computed as strain of the metastatic vertebra normalised with respect to the healthy vertebra. Scans in the unloaded condition and at failure were rigidly registered and overlapped to identify the location of failure onset and the failure mode of metastatic and control vertebrae.

Results

SDER for healthy and metastatic vertebrae were similar, and below 500µε. Vertebrae with lytic metastases experienced the largest eps3 at failure (median ± standard deviation over the entire vertebral body: -8506 ± 4748 µε), followed by vertebrae with mixed metastasis (-7035 ± 15605 µε), healthy vertebrae (-5743 ± 5697 µε) and with blastic metastases (-3150 ± 4641 µε) (Fig. 1).
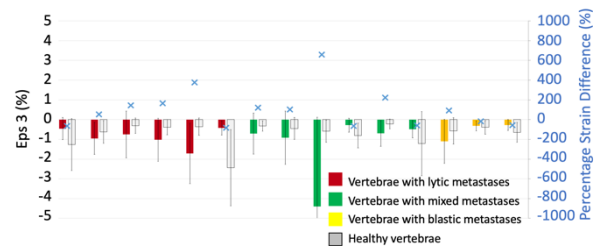

Fig. 1: strain over the vertebral body for each vertebra (median and SD) and percentage strain differences for each spine segment.

In the segments with lytic or mixed metastases, the vertebra with metastases failed first in 4/6 or 5/6 cases, respectively. In segments with blastic metastases the metastatic vertebra failed only in 1/3 cases. Onset failure location was near the endplates. In vertebrae with lytic metastases, the failure occurred between the endplate and the metastatic lesions, while in vertebrae with blastic metastases the failure occurred around the metastatic lesion (Fig. 2).
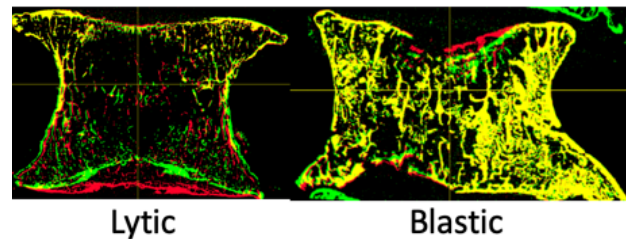

Fig. 2: failure pattern in vertebrae with lytic and blastic metastases. Vertebra before (red) and after (green) the failure. In yellow, overlapped regions

Discussion

Each type of lesion affected the strain of the internal tissue in a different way, making it essential to assess in detail the properties of the lesion, the bone microstructure, and the local tissue deformation in each case. Vertebrae with lytic and mixed lesions showed the largest deformations and high likelihood of fracture compared to the adjacent healthy control (Percentage Strain Differences, Fig. 1). Blastic metastasis can lead to failure of the affected vertebra or of the adjacent healthy one.

References

1. Stadelmann et al., (2020), *Bone*
2. Palanca et al. (2021), *Bone*
3. Dall'Ara and Tozzi (2022), *Front Bioeng Biotech*
4. Dall'Ara et al., (2014), *J Biomech*

Acknowledgements